In situ root identification through blade penetrometer testing – Part 2: field testing

G. J. Meijer*†‡§ A. G. Bengough*† J. A. Knappett* K. W. Loades†
B. C. Nicoll‡

Published in: Géotechnique 68(4), 320–331 (2018). DOI:10.1680/jgeot.16.P.204

Abstract

The spatial distribution, depths and diameters of roots in soil are difficult to quantify but important to know when reinforcement of a rooted slope or the stability of a plant is to be assessed. Previous work has shown that roots can be detected from the depth–resistance trace measured using a penetrometer with an adapted blade-shaped tip. Theoretical models exist to predict both forces and root displacements associated with root failure in either bending or tension. However, these studies were performed in dry sand under laboratory conditions, using acrylonitrile butadiene styrene root analogues rather than real roots. In this paper blade penetrometer field testing on two forested field sites, with Sitka spruce and pedunculate oak in sandy silt and clayey silt respectively, is used to evaluate models under field conditions. Root breakages could be detected from blade penetrometer depth–resistance traces and using complementary acoustic measurements. Predictions of additional penetrometer resistance at root failure were more accurate than the displacement predictions. An analytical cable model, assuming roots are flexible and fail in tension, provided the best predictions for Sitka roots, while thick oak roots were better predicted assuming bending failure. These matched the modes of failure observed in 3-point bending tests of the root material in each case. The presence of significant amounts of gravel made it sometimes difficult to distinguish between hitting a root or a stone. The root diameter could be predicted when root strength and stiffness, and soil penetrometer resistance were known and the right interpretative model selected. Estimates based on peak force were more accurate than those based on root displacement. This measurement procedure is therefore a potentially valuable tool to quantify the spatial distribution of roots and their reinforcement potential in the field.

KEYWORDS: environmental engineering; in situ testing; penetrometers; slopes; vegetation

1 Introduction

Vegetation can reinforce soil and help to stabilise slopes (Coppin and Richards, 1990; Gray and Sotir, 1996). Roots increase the shear strength of the soil through mobilising tension or bending forces in the root. To quantify this effect, information is required about the spatial distribution, depths, diameters and mechanical properties of the roots. Gathering these requires extensive and time-consuming field work, often including sampling or digging of trenches or pits.

Blade penetrometer testing as a method to quantity root depths and diameters, which does not require digging or sampling, was first introduced by Meijer et al. (2016) and subsequently tested in idealised laboratory conditions (Meijer et al., 2017). Both studies, using acrylonitrile butadiene

*University of Dundee, Division of Civil Engineering, Dundee DD1 4HN, UK
†James Hutton Institute, Invergowrie, Dundee DD2 5DA, UK
‡Forest Research, Northern Research Station, Roslin, Midlothian EH25 9SY, UK
§Corresponding author, g.j.z.meijer@dundee.ac.uk

styrene (ABS) root analogues, showed that the penetrometer resistance increased gradually once a root gets caught by the penetrometer tip until the moment of root failure, visible as a sudden rapid decrease in force. This distinct shape in the depth–resistance trace is hereafter referred to as a 'root peak'. Meijer et al. (2017) showed that when root material strength and stiffness as well as root resistance are known, the diameter of the root can be predicted from the measured depth–resistance trace. The additional penetrometer resistance introduced by a single root just before it breaks ('peak root resistance' F_u) was accurately estimated for the ABS root analogues, which broke in bending. Predictions for the associated penetrometer displacement required to break the root from the moment it is first touched ('peak root displacement' u_u) were shorter than measured.

Real roots however are often weaker and more flexible than ABS (Meijer et al., 2016) and the variation in real root tensile strength and stiffness is large. Generally, thin roots are found to be stronger than thicker roots (e.g. Mao et al., 2012). Data on tree root stiffness is scarce, but has been recorded in a number of studies (Waldron and Dakessian, 1981; Operstein and Frydman, 2000; Van Beek et al., 2005; Fan and Su, 2008; Mickovski et al., 2009; Loades et al., 2013). Generally only tensile properties are studied, neglecting root bending behaviour.

Trees can develop plate root systems (many lateral roots plus vertical sinker roots), heart root systems (horizontal, oblique and vertical roots) or tap root systems (large central vertical root with smaller laterals; Gray and Sotir, 1996; Stokes et al., 2009), depending on species, soil and environmental conditions (Coppin and Richards, 1990; Stokes et al., 2009). Most tree roots occur in the surface soil horizons (Jackson et al., 1996; Bischetti et al., 2005) as many tree roots grow horizontally. This is especially the case when the bedrock is shallow, the water table in the soil is high or when there is a dense layer of soil that restricts root penetration.

In this paper, the blade penetrometer methodology developed by Meijer et al. (2017) was tested *in situ* in two forests with different soil conditions and tree types. The results are compared to several analytical interpretative models, based on root tensile or bending failure. Thus the suitability of the methodology and interpretative methods was assessed under field conditions.

2 Methods

2.1 Field sites

Field testing was performed on two different sites with contrasting soil and root types. The first was Hallyburton Hill forest, a Forestry Commission owned woodland in the Sidlaw Hills, near Dundee, UK (56°31'10.3"N, 3°11'29.9"W), planted in 1961 with Sitka spruce (*Picea sitchensis*), see Figure 1a. Sitka spruce is the most common conifer in UK woodlands, accounting for 51% of the growing stock (Forestry Commission, 2015). The soil was classified as sandy silt and is henceforth referred to as 'Sitka spruce forest'. The second site was Paddockmuir Wood, a Forestry Commission owned woodland near St Madoes, UK (56°21'55.3"N, 3°16'13.0"W), planted with mature pedunculate oak (*Quercus robur*) and interspersed with young Sycamore (*Acer pseudoplatanus*), see Figure 1b. Oak is the most common broadleaf in UK woodlands (16%); only birch is grown more (18%) (Forestry Commission, 2015). The soil was classified as clayey silt and is is henceforth referred to as 'oak forest'.

Soil dry densities and water contents were measured for multiple replicates using 100 cm^3 ring samples, collected within 0.5 m of the closest blade penetrometer measurement location at both sites. Soil suctions were measured in situ using field tensiometers (model SWT4, Delta-T). Horizon depths were manually determined from visual observation in soil pits and compared with the Soil Information for Scottish Soils database (James Hutton Institute, 2016). Results for both sites can be found in Figure 2. Particle size distributions for both field sites and the sand used in Meijer et al. (2017) can be found in Figure 3. The two field sites strongly contrast with the dry uniform fine sand used in the laboratory tests (Meijer et al., 2017). The densities at both sites are looser than those tested in the laboratory (approximately 1.63 Mgm^{-3} and 1.72 Mgm^{-3} for the 50% and 80% relative density

(a) Sitka spruce at Hallyburton Hill.

(b) Oak tree at Paddockmuir Wood.

Figure 1: Pictures of field sites.

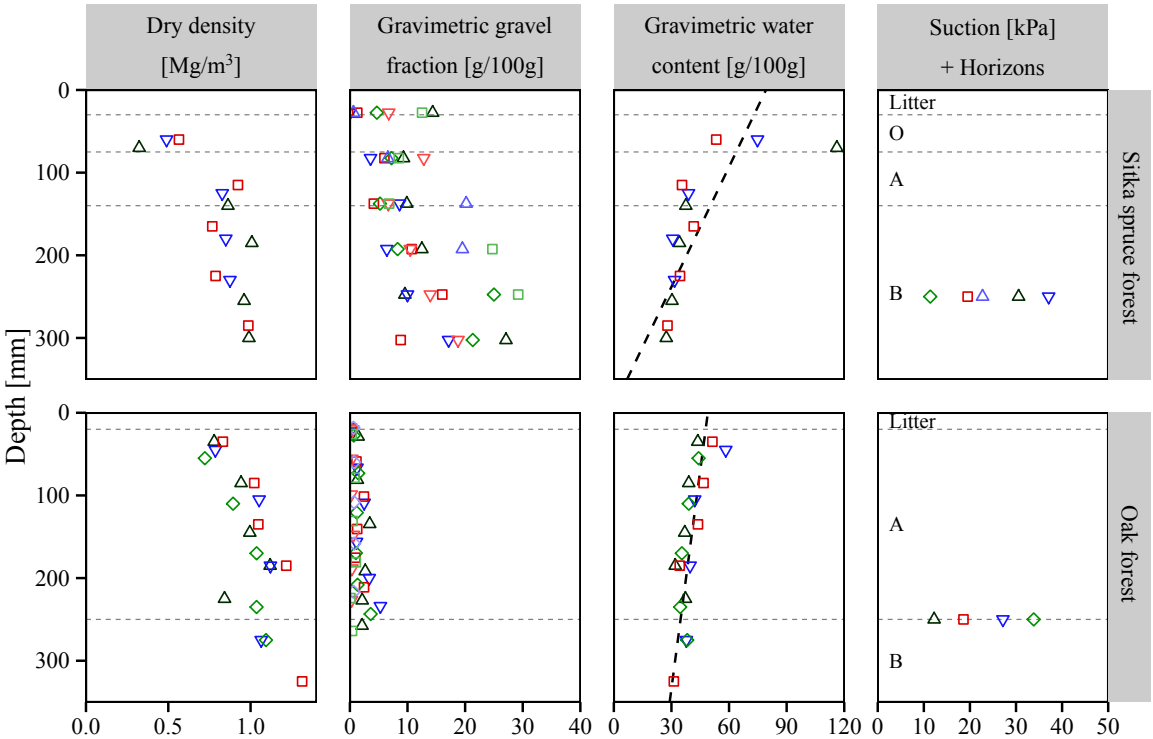

Figure 2: Soil properties for blade penetrometer testing at both field sites. Different markers indicate replicates.

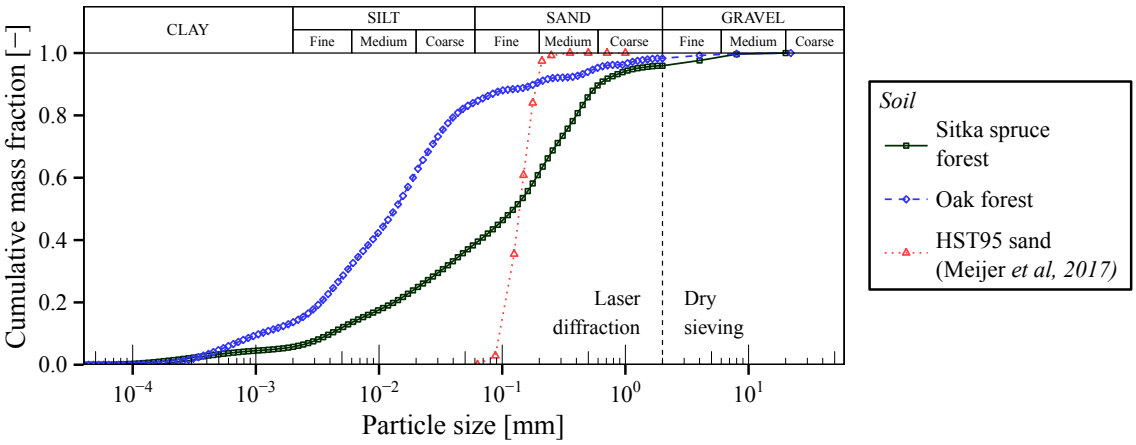

Figure 3: Particle size distributions for soils used in this study. Laser diffraction (British Standards Institution, 2010) was used to quantify the amount of particles smaller than 2 mm, while dry sieving was adopted for particles > 2 mm. Field soils were sampled between 150 and 250 mm depth. Particle sizing for (laboratory) HST95 sand was determined using dry sieving only, see Lauder (2010).

sands, respectively).

2.2 Root mechanical characteristics

Root strength and stiffness were determined from tensile tests and 3-point bending tests. Intact root diameters (d_r) were measured using a microscope fitted with an eyepiece graticule.

Seventy-six Sitka and 53 Oak samples with a length of 100 mm were tested in tension using a loading rate of 5% strain per minute (5 mm min^{-1} for 100 mm long roots), in line with loading rates reported in literature (1–10 mm min^{-1}, e.g. Genet et al. (2008); Loades et al. (2010)). A further 24 shorter oak samples (60 mm long) were tested at the same strain rate. Roots were clamped by hydraulic clamps using 100–300 kPa of pressure, with more pressure used for thicker roots. For roots thicker than approximately 3 mm, the bark was stripped near the clamps to ensure good grip between the clamps and the root stele (the core part of the root beneath the outer bark). The presence of the bark was not expected to influence the tensile strength, as during tests it cracked and peeled prior to reaching the peak tensile strength, i.e. failing well before the stele. The root diameter range tested in tension was 0.39–10.2 mm for Sitka spruce and 0.48–9.1 mm for oak roots

Eighty-two Sitka and 53 Oak samples were tested using three-point bending tests, loaded at 5 mm min^{-1} to a maximum deflection of 50 mm. The span length was varied so that it exceeded $10 \cdot d_r$ to minimise the effects of shear on the results. Only for the two thickest oak ($d_r > 11$ mm) and Sitka samples ($d_r > 25$ mm) this ratio was slightly smaller (7.5–8.5) due to limited root length. Although a value of $L/d_r = 20$ is recommended for testing of wood and timber (Rowe et al., 2006), root lengths were insufficient to satisfy this due to limited root lengths which could be collected or changing root properties over the length of the root, e.g. excessively tapered or twisted roots. The constant displacement rate meant that rates of bending strain in the root varied with root diameter and span length between approximately 0.9 and 6.0% strain per minute. The diameter range of roots tested in tension was 0.52–26.5 mm for Sitka spruce and 0.35–13.3 mm for oak roots.

Two stiffnesses were measured: the initial tangent stiffness (Young's modulus, E) and the secant stiffness at 90% of peak strength (E_{90}). The secant stiffness is more useful when the root is modelled using linearised elasticity, as it represents a better fit to non-linear root stress–strain behaviour compared to the Young's modulus (Figure 4). Strength and stiffness parameters were fitted using exponential curves commonly adopted in root research (e.g. Mao et al., 2012):

$$\sigma = \alpha_\sigma \cdot d_r^{\beta_\sigma} \tag{1}$$

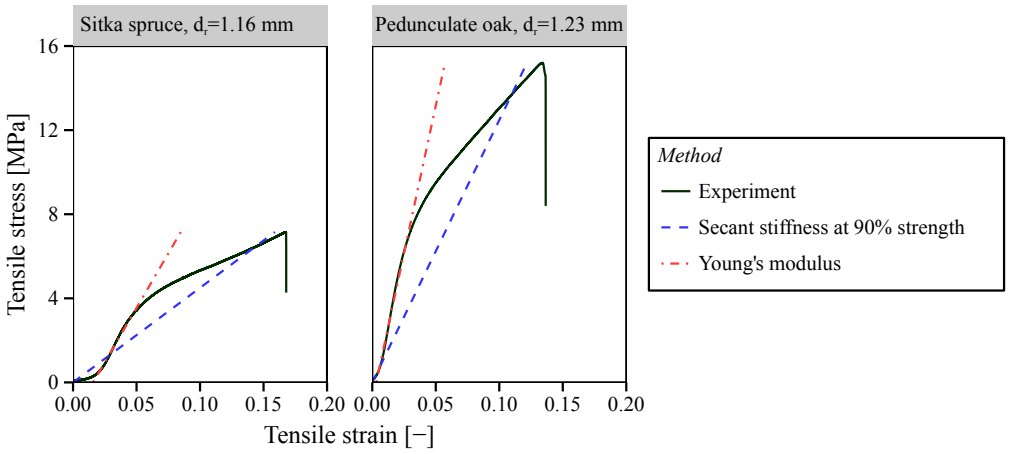

Figure 4: Example stress–strain curves for roots of similar diameter tested in uniaxial tension.

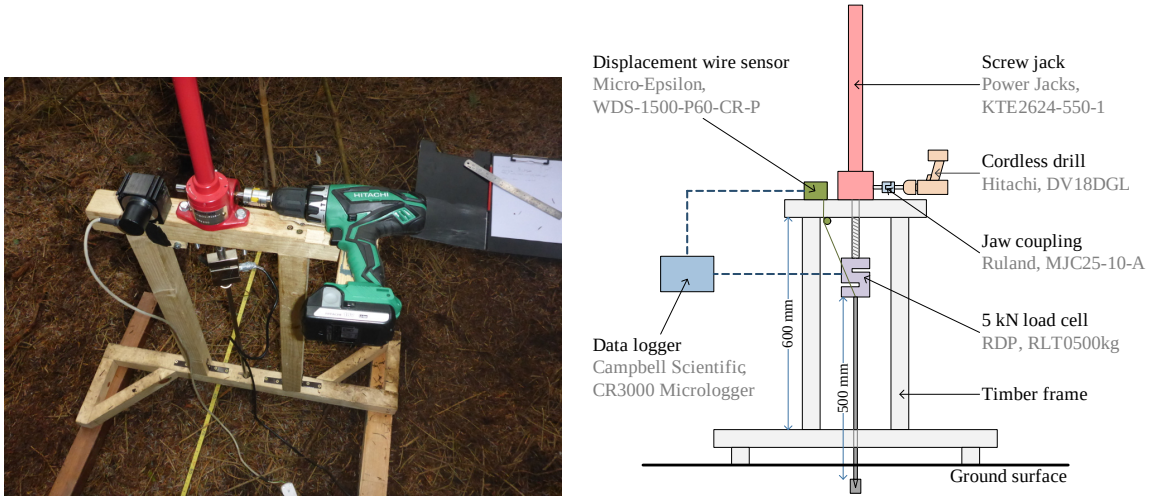

(a) Picture of the setup at the Sitka spruce forest

(b) Schematic.

Figure 5: Blade penetrometer field measurement setup.

$$E = \alpha_E \cdot d_r^{\beta_E} \tag{2}$$

where α and β are fitting parameters.

2.3 Field penetrometer testing

The blade penetrometer shape was similar to that used by Meijer et al. (2016), i.e. a 30×2×38 mm (width × depth × height) blade welded to a ∅12 mm 30° cone and connected to a 500 mm long ∅10 mm shaft. This shaft was connected via a 5 kN load cell to a screwjack. The screwjack was powered by a battery powered power drill (55 Nm maximum torque) to maintain a constant penetration rate. The resulting penetration rate was approximately 150 mm min^{-1}, of the same order of magnitude as the 300 mm min^{-1} used in previous laboratory testing (Meijer et al., 2017, 2016). Details and a picture of the setup can be found in Figure 5. Force and displacement were measured at 100 Hz using a data logger (CR3000 Micrologger, Campbell Scientific). The body mass of two operators, one on each side of the frame, provided a reaction force. At each site, 8 tests were performed.

Additional penetrometer tests were performed using a standard agricultural penetrometer tip (∅12 mm 30° cone on a ∅10 mm shaft, henceforth referred to as 'standard penetrometer') mounted on the same frame. In the Sitka spruce forest three, and in the oak forest four successful traces were collected.

In the oak forest, all tests were performed between 0.7 and 1.5 m distance to a dominant oak tree

(diameter at breast height: 770 mm) to ensure roots would be encountered. In the Sitka spruce forest, tests were performed within tree rows, with distances to the nearest tree ranging between 0.5 and 1.4 m. The maximum penetration depth was approximately 300 mm at the oak forest and 350 mm at the Sitka spruce forest. Below these depths, soils were too stony for penetration.

In the blade penetrometer tests in the oak forest an acoustic microphone (Genius Multimedia Microphone MIC-01A) was placed in the soil 100 mm deep, at approximately 150 mm from the test location, to record sounds of root breakage (similar to Coutts, 1983). Coutts used multiple microphones to identify the location of breaking roots during the overturning of trees. Here the aim is to study whether it is possible to identify root breakage due to penetrometer action.

2.4 Root and stone measurements

On both sites, a large core sampler (height 110 mm, diameter 100 mm) with a cutting rim and three 20 mm high cutting edges was used to extract large soil cores at the location of each blade penetrometer test. A large ∅100 mm metal spike in the centre of the corer helped to keep the sampler in line with the hole left by the penetrometer. The extracted cores were frozen after sampling and horizontally split in two using a diamond saw. The total dry mass of these cores was determined by weighing the frozen core and using the (fitted) soil water content measured using the 100 cm^3 cores (see Figure 2 for the adopted fits). Roots broken by the blade penetrometer could be detected during gentle washing with warm water on a 2 mm sieve. A root was classified as broken when the breakage occurred in the middle of the core. Breakages within 20 mm of the core side were assumed to be created by the sampling procedure. The depths of these roots were recorded and their diameters measured using a microscope fitted with an eyepiece graticule. Roots extracted from core samples were scanned and their diameters and lengths analysed using WinRhizo (Regent Instruments, version 2003b), using 0.1 mm wide diameter classes. During root washing, soil particles > 2 mm were collected and subsequently dried and sieved using 2, 4, 8 and 22 mm sieves.

2.5 Data processing

In the measured depth–resistance profiles, the peak root resistance (F_u) could be identified from the sudden drop in blade penetrometer resistance (Figure 6). The drop in resistance was attributed to a root when:

- Resistance continuously decreased over the whole range of the drop.
- Resistance drops were at least 2 N, and at least 4 times larger than the median value of drops encountered in a zone of 2 mm above and below the drop. This filters out drops introduced by signal noise without smoothing out potential force drops introduced by roots.
- The gradient of the drop in resistance resistance was larger than 200 Ns^{-1} (or approximately 80 Nmm^{-1} since test were conducted in a displacement-controlled fashion).
- The resistance does not rapidly increase before or after the potential drop. This filters out electrical noise spikes in the measurements.

Numerous peaks were identified this way. For every drop, roots identified as broken during washing were associated with this drop when the root depth was within a 20 mm distance of any point on the the force peak. A margin was required since core sampling did not always provide good quality cores, introducing uncertainty in the actual root depth. When it was unclear at which depth resistance started to increase due to the presence of a root, this depth was estimated using $z_0 = z_1 - \alpha_f \cdot \Delta F$, where z_0 and z_1 are the depths associated with the start of the peak and the peak root resistance, ΔF the magnitude of the peak root resistance and α_f the gradient (assumed to be 15 Nmm^{-1} for the Sitka spruce forest and 10 Nmm^{-1} for the oak forest). Values for α_f were based on peaks which could easily be identified. Where single or multiple root peaks for each root could be related to single or multiple roots the most likely root peak candidate was selected based on the shape of the peak and visual observations of broken root ends.

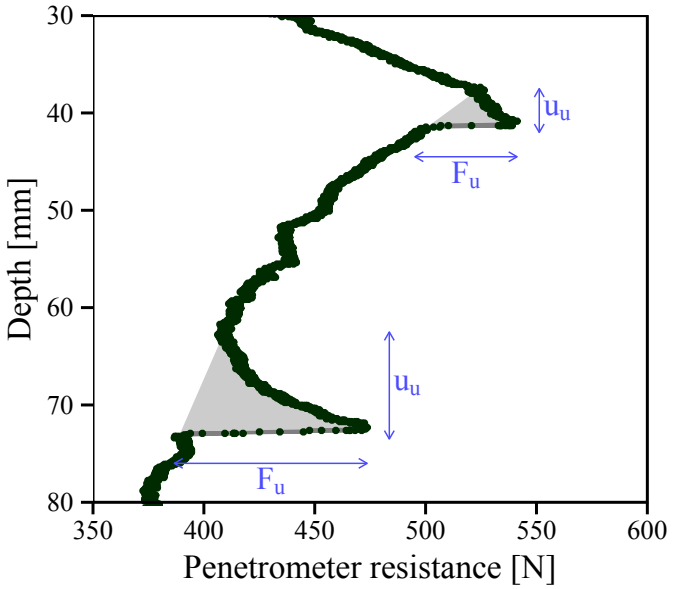

Figure 6: Example of increases in penetrometer resistance (grey shaded zones) caused by individual roots. Excerpt from test 8 performed in the oak forest.

2.6 Interpretative models

Predictions of the root diameter were made for every broken root within 20 mm of an identified resistance peak, based on either measured peak root resistance F_u or peak root displacement u_u, after Meijer et al. (2017):

(i) When roots are assumed to break in bending, the penetrometer force required to break the root ($F_{u,b}$ [N]) was:

$$F_{u,b} = 1.0231 \cdot d_r^2 \cdot \sqrt{\sigma_b \cdot p_u}, \quad \text{i.e. } d_r \approx \frac{\sqrt{F_{u,b}}}{\sqrt[4]{\sigma_b \cdot p_u}} \tag{3}$$

and the corresponding root displacement ($u_{u,b}$ [mm]):

$$u_{u,b} = 0.09808 \cdot d_r \cdot \frac{\sigma_b^2}{E_b \cdot p_u}, \quad \text{i.e. } d_r \approx 10 \cdot \frac{u_{u,b} \cdot E_b \cdot p_u}{\sigma_b^2} \tag{4}$$

where d_r is the root diameter [mm], σ_b the bending strength [MPa], E_b the bending stiffness [MPa] and p_u the soil resistance [MPa].

(ii) When roots are assumed to break in tension, the peak root resistance ($F_{u,t}$ [N]) is:

$$F_{u,t} = \frac{\pi}{4} \cdot d_r^2 \cdot \sigma_t \cdot \frac{4 \cdot \sqrt{\eta}}{1+\eta}, \quad \text{i.e. } d_r = \sqrt{\frac{F_{u,t}}{\pi \cdot \sigma_t}} \cdot \frac{\sqrt{\eta+1}}{\sqrt[4]{\eta}} \tag{5}$$

and the corresponding displacement ($u_{u,t}$ [mm]):

$$u_{u,t} = \frac{\pi}{4} \cdot d_r \cdot \frac{\sigma_t}{p_u} \cdot \sqrt{\zeta}, \quad \text{i.e. } d_r = \frac{4}{\pi} \cdot u_{u,t} \cdot \frac{p_u}{\sigma_t \cdot \sqrt{\zeta}} \tag{6}$$

where σ_t is the tensile strength [MPa] and E_t the tensile stiffness [MPa]; ζ [-] and η [-] are defined as:

$$\eta = \sqrt{\frac{\zeta + 2 \cdot \sqrt{\zeta+1} + 2}{\zeta}} \tag{7}$$

$$\zeta = \frac{1}{8} \cdot \frac{\sigma_t \cdot p_u}{E_t \cdot \tau_i} \tag{8}$$

where τ_i [MPa] is the interface friction between the root and the surrounding soil.

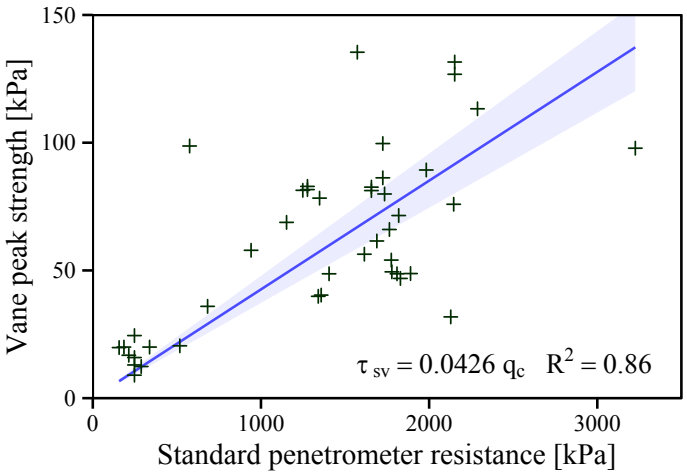

Figure 7: Correlation between peak vane shear strength and standard penetrometer resistance in the Sitka spruce forest.

Both models (i) and (ii) require an estimate of the soil resistance parameter p_u (essentially the ultimate capacity of a p-y curve used to model the root–soil interaction). These estimates were based on the blade penetrometer resistance just after the root had broken (F_{blade}). The blade penetrometer resistance was multiplied by a factor α_1 to find the equivalent force for the standard penetrometer. This value was divided by the standard penetrometer tip area ($A_{std.tip}$) to find standard penetrometer resistance q_c [MPa]. The value for α_1 was found by comparing the average in situ measured blade penetrometer and standard penetrometer traces. Because the shape of the standard penetrometer (conical) was different from the root (circular), a second factor α_2 was required to estimate p_u. Here $\alpha_2 = 0.623$, based on comparing penetrometer results with Reese and Van Impe (2011)'s method in dry sandy soil in laboratory testing (Meijer et al., 2017). Thus:

$$p_u \approx \frac{F_{blade} \cdot \alpha_1}{A_{std\,tip}} \cdot \alpha_2 = q_c \cdot \alpha_2 \tag{9}$$

Furthermore, the tensile model requires an estimate for the soil–root interface friction (τ_i). For the Sitka spruce forest, this value is based on an experimentally determined linear relation (in terms of $y = a \cdot x$) between vane shear strength in the soil (τ_{sv} [MPa], measured using a 50×34 mm cruciform blade, Pilcon hand vane) and standard penetrometer resistance (q_c [MPa]), see Figure 7:

$$\tau_{sv} \approx 0.0426 \cdot q_c,\ R^2 = 0.86 \tag{10}$$

To compensate for the root–soil interface friction being smaller than the soil–soil friction, the soil frictional strength is reduced by a factor $f = 0.5$ (Gray and Sotir, 1996). Combining equations 9 and 10 gives:

$$\tau_i = f \cdot \tau_{sv} \approx 0.0426 \cdot f \cdot \frac{F_{blade} \cdot \alpha_1}{A_{std\,tip}} \tag{11}$$

Equation 11 was also used for the oak forest because no penetrometer versus shear strength dataset was available.

(iii) The third and final model used assumed that the peak root resistance is equal to twice the root tensile strength, and was only used to make predictions based on magnitude of the peak root resistance and not from the peak displacement. This model assumed the root resistance is independent from the soil behaviour, and can be seen as a particular case of the analytical cable model where $\zeta \to \infty$, i.e. where the root is extremely flexible compared to the soil:

$$F_{u,\sigma_t} = 2 \cdot \frac{\pi}{4} \cdot d_r^2 \cdot \sigma_t \tag{12}$$

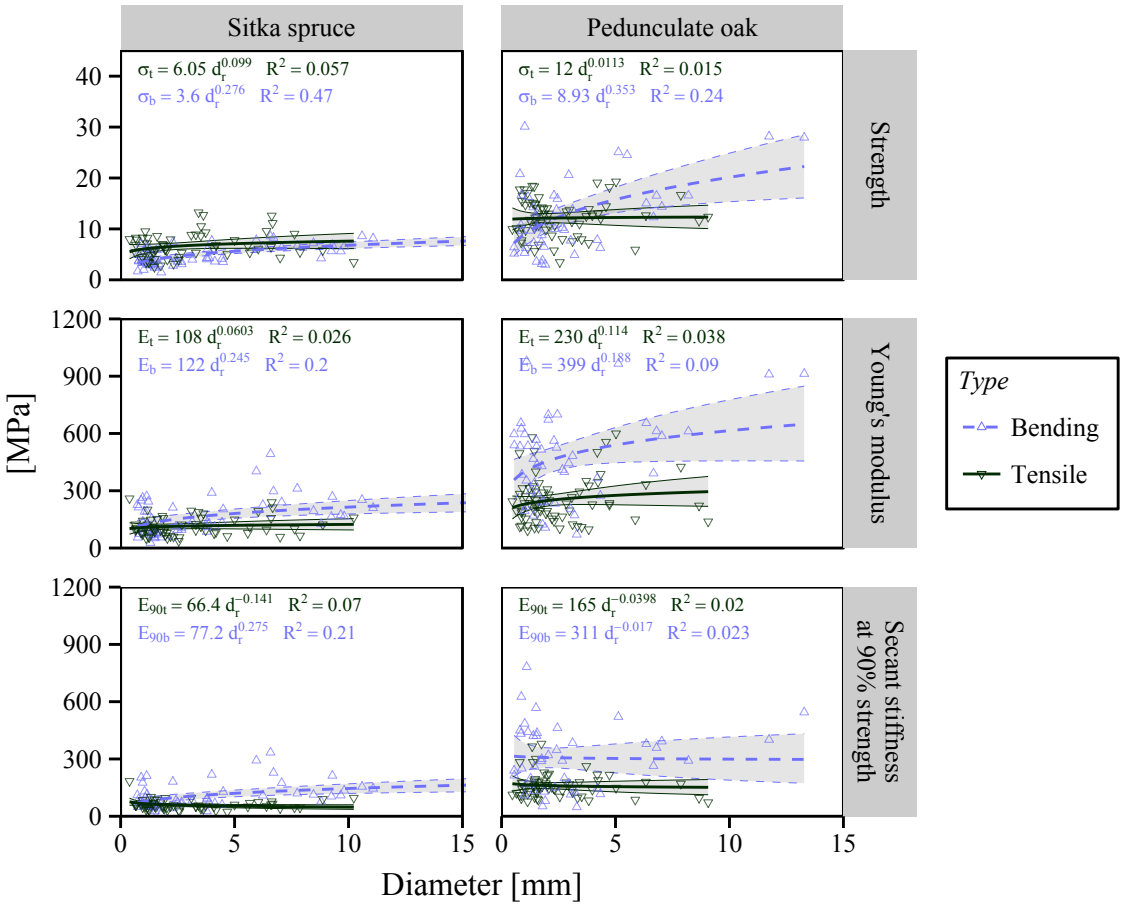

Figure 8: Root tensile and bending strength and stiffnesses for Sitka spruce roots and pedunculate oak roots. The lines indicate the best power law fit and 95% confidence interval of the fit parameters. All fits are plotted despite some having non-significant power coefficients (β) , see text.

3 Results

3.1 Root mechanical characteristics

Tensile and 3-point bending tests for both species showed weak strength–diameter and stiffness–diameter relationships (Figure 8). R^2 values were small, showing little diameter dependence. Fitted power coefficients in the tension tests all were close to zero. The only statistically significant ($p \leq 0.05$) trend in tension was found for E_{90} for Sitka spruce (negative power). All power coefficients were positive and statistically significant in bending tests, apart from E_{90} measured for oak roots.

The ratio between the secant stiffness at 90% strength (E_{90}) and Young's modulus (E) was on average 0.648 ± 0.020 (mean $\pm$ standard error, tension) and 0.558 ± 0.020 (bending) for Sitka spruce roots. For oak roots, these ratios were 0.708 ± 0.025 and 0.778 ± 0.043 respectively. This showed root stress–strain behaviour is considerably non-linear.

None of the Sitka roots broke in bending despite significant post-peak strain. They behaved more like a bundle of fibres where the fibres realigned rather than ruptured. The material on the concave side buckled (Figure 9a), suggesting that the root will not snap in pure bending. In contrast, in three out of seven bending tests on thick oak roots ($d_r > 6$ mm) tensile failure was observed on the convex side (Figure 9b).

(a) Sitka spruce root (bark stripped to facilitate observation)

(b) Pedunculate oak root

Figure 9: Pictures of three-point bending tests. The scale at the bottom has 1 mm increments.

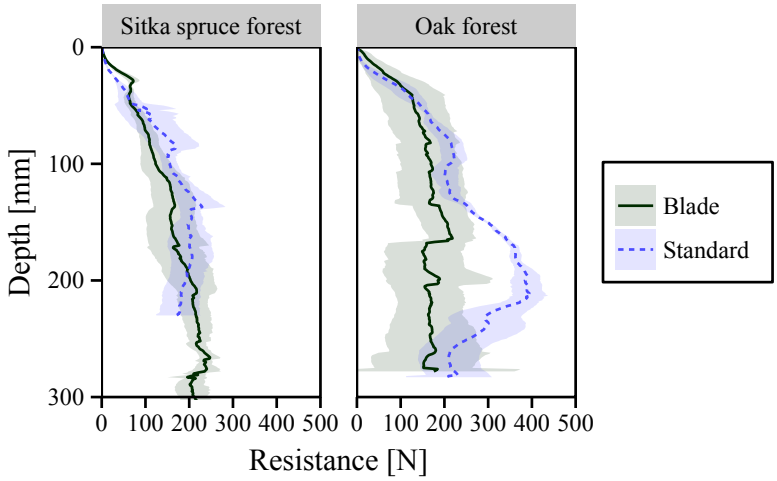

Figure 10: Average blade penetrometer and standard penetrometer resistance for both sites. The shaded area indicates the mean resistance ± one standard error for each depth level.

3.2 Penetration resistances – determination of α_1

The blade penetrometer resistance is generally higher than the standard cone penetrometer resistance (Figure 10). Between 10 and 150 mm depth, the blade penetrometer resistance force was approximately 70% greater (Sitka spruce forest: 72%, Oak forest: 67%). For modelling purposes it was assumed that $\alpha_1 \approx 0.588$ (Figure 11). The standard penetrometer resistance in the oak forest was relatively greater at 150–250 mm depth, probably due to variation in the soil structure and properties between the two test locations (the oak forest was considerably more variable than the Sitka spruce one). Below 250 mm depth the ratio between standard and blade penetrometer resistance reverts back to approximately $\alpha_1 = 0.588$. Neither the blade penetrometer traces nor visual inspection of and soil horizons explained this increased resistance.

3.3 Blade penetrometer results

Blade penetrometer traces for both sites are presented in Figures 12 and 13. The data for Test 5 in the oak forest was discarded because of faulty datalogger force measurements over part of the trace. Traces at the Sitka spruce forest (5, 7, 8) and oak forest (2, 3, 4) exceeded the maximum penetration force before the target depth was reached. Many of the identified root peaks measured in the oak forest were accompanied by a short spike in sound amplitude. The short duration (typically in the

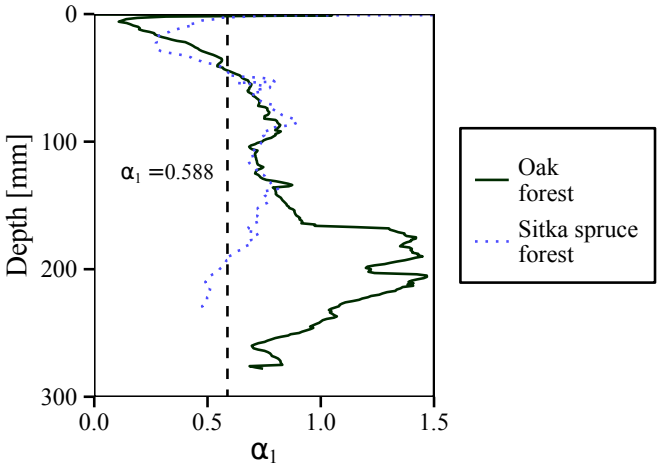

Figure 11: Ratio between standard and blade penetrometer resistance (force) α_1 as function of depth.

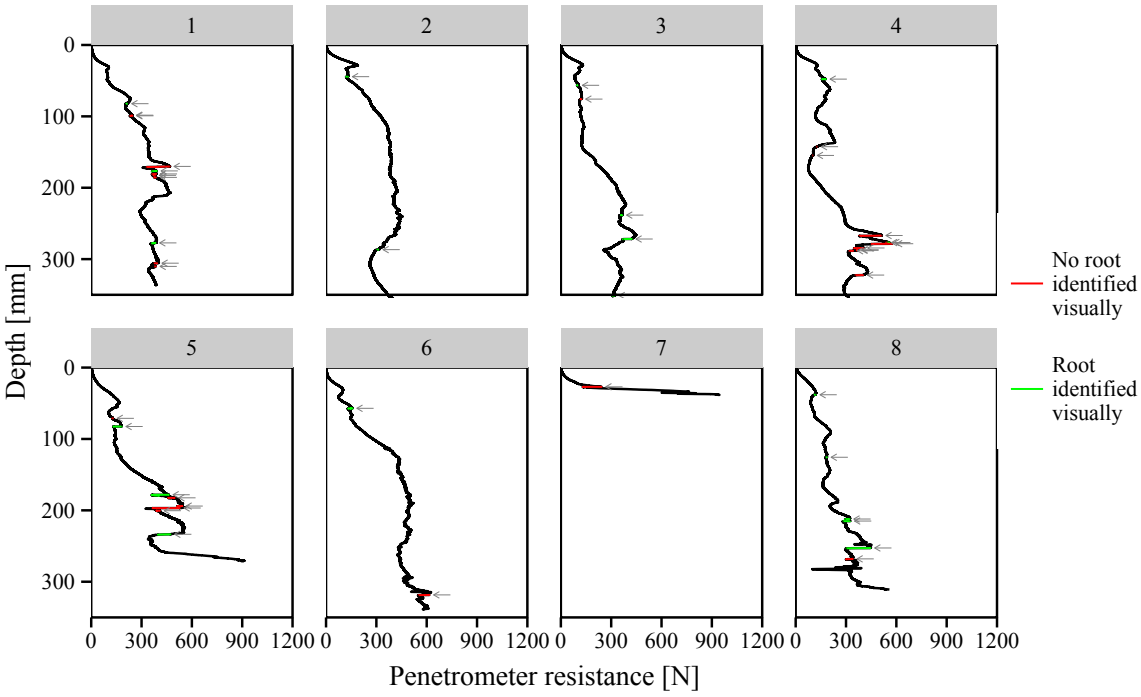

Figure 12: Blade penetrometer traces measured in the Sitka spruce forest. Sudden drops in penetrometer resistance are indicated in the graph with arrows. Colours indicate whether a drop could be associated with a root.

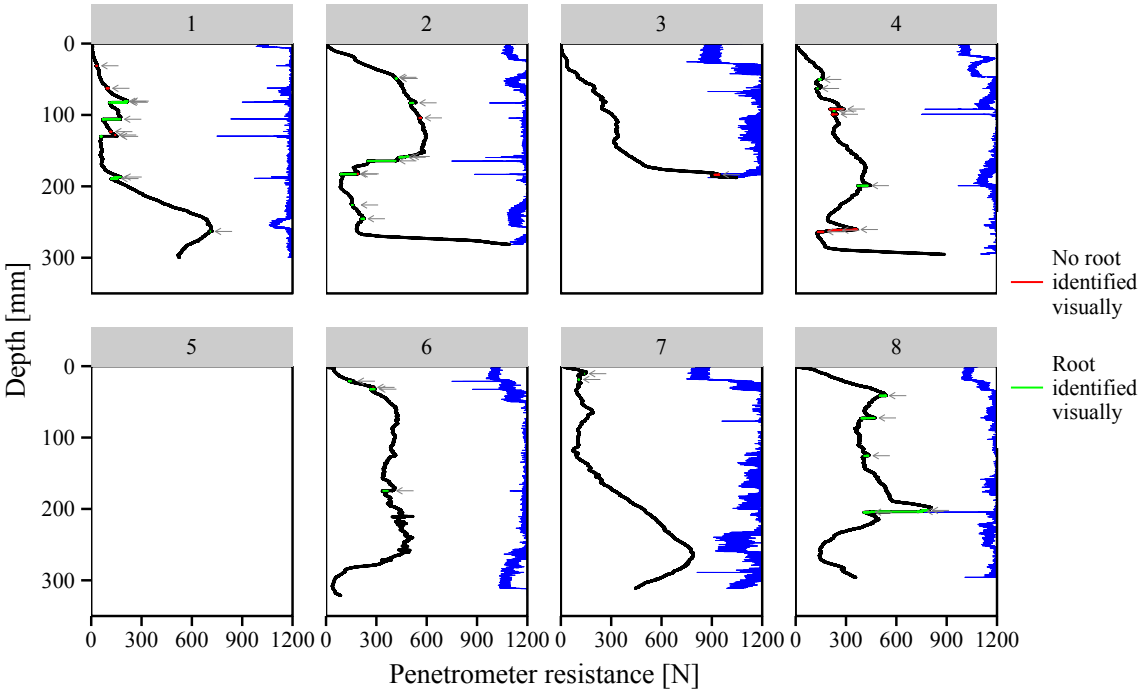

Figure 13: Blade penetrometer traces measured in the oak forest. Sudden drops in penetrometer resistance are indicated in the graph with arrows. Colours indicate whether a drop could be associated with a root. Blue traces (on the right of each plot window) are scaled $\log_{10}$-transformed measurements of the absolute sound amplitude.

order of hundreds of milliseconds) is considered to be indicative of root breakage. Uniaxial tensile testing showed that root failure is brittle and occurs fast. It is hypothesised that if the resistance change was caused by stones, longer sound peak durations would have been expected as scraping between stone and penetrometer occurs while the stone is gradually pushed aside.

The results for diameter predictions based on either the peak root resistance or peak root displacement are presented in Figures 14 and 15 for the Sitka spruce forest and Figures 16 and 17 for the oak forest. For the Sitka spruce forest, the best diameter predictions based on peak root resistance were made using the cable model. These predictions are close to the simple $2\times$ tensile strength approximation, indicating that the roots are flexible with respect to the soil resistance. The same holds true for predictions based on peak root resistance measured in the oak forest, but only for thin roots ($d_r \leq 2$ mm). The measured diameter for thicker oak roots lay somewhere between tensile and bending predictions. These observations were consistent with the root failure modes observed in the three-point bending tests (Figures 9a and 9b), suggesting that thicker oak roots often fail in bending while Sitka spruce roots are unlikely to.

Predicted diameters based on the bending model displacement proved to be extremely inaccurate for both sites. Predictions based on displacement were more accurate when the cable model was used, especially for thin roots ($d_r < 2$ mm). However, for thicker roots the predicted diameter using the cable model was significantly smaller than measured. Diameter predictions based on peak root displacement were more scattered than those based on peak root resistance.

4 Discussion

No root strength or stiffness data was found in the literature for pedunculate oak. For Sitka spruce, some limited data on averaged tensile properties is available. Coutts (1983) reported tensile strengths

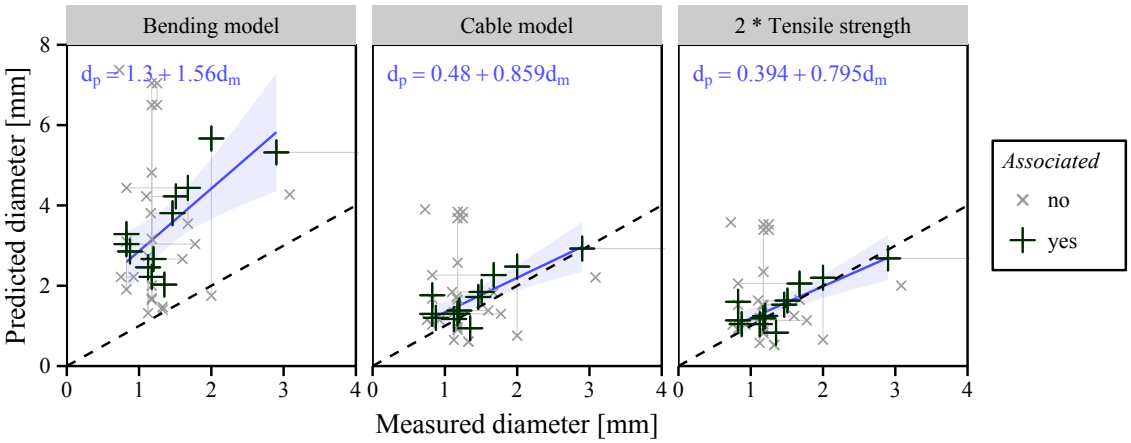

Figure 14: Diameter prediction based on peak root resistance measured in the Sitka spruce forest. 'Associated' data points indicate the manually selected most likely combinations of root and measured peak root resistance. Other points indicate all other possible combinations of root and peak resistance. Combinations belonging to the same root or peak root resistance are connected by vertical and horizontal lines respectively.

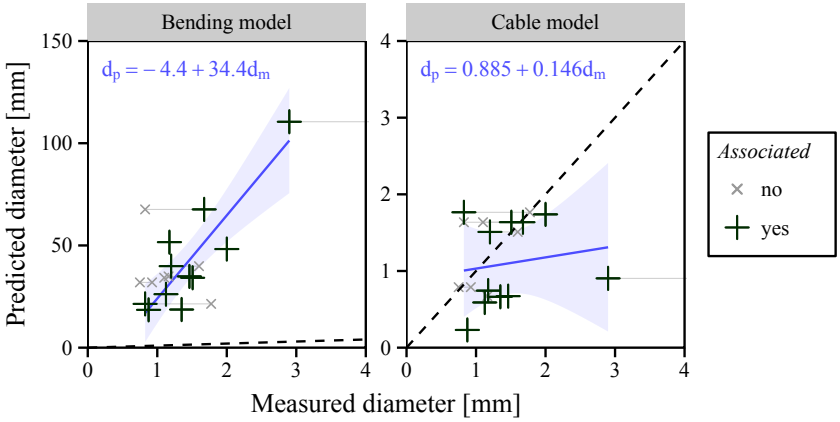

Figure 15: Diameter prediction based on peak root displacement measured in the Sitka spruce forest. 'Associated' data points indicate the manually selected most likely combinations of root and measured root peak. Other points indicate all other possible combinations of root and peak root displacement. Combinations belonging to the same root or root peak are connected by vertical and horizontal lines respectively.

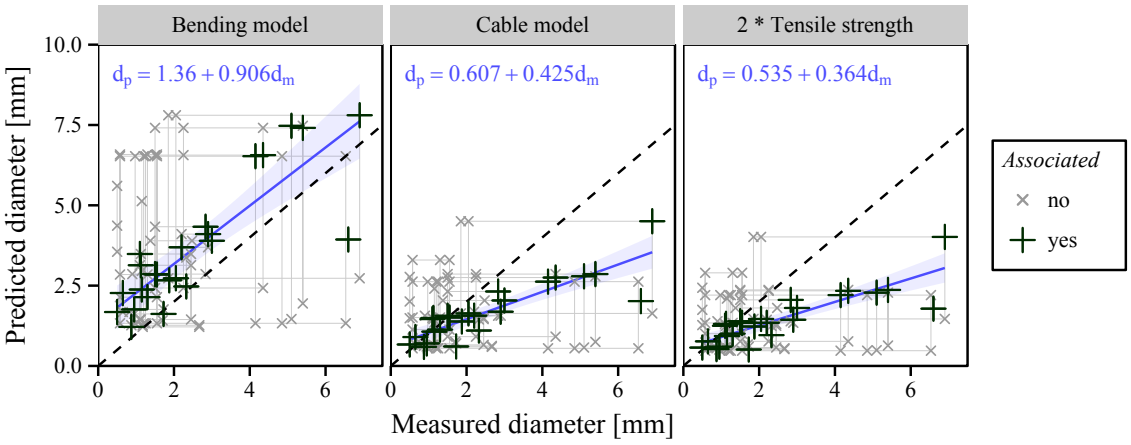

Figure 16: Diameter prediction based on peak root resistance measured in the oak forest. 'Associated' data points indicate the manually selected most likely combinations of root and measured root peak. Other points indicate all other possible combinations of root and peak root resistance. Combinations belonging to the same root or root peak are connected by vertical and horizontal lines respectively.

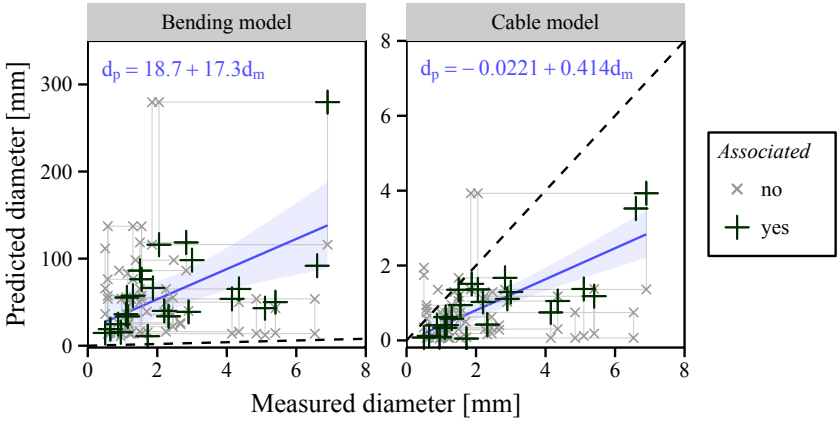

Figure 17: Diameter prediction based on peak root displacement measured in the oak forest. 'Associated' data points indicate the manually selected most likely combinations of root and measured root peak. Other points indicate all other possible combinations of root and peak root resistance. Combinations belonging to the same root or root peak are connected by vertical and horizontal lines respectively.

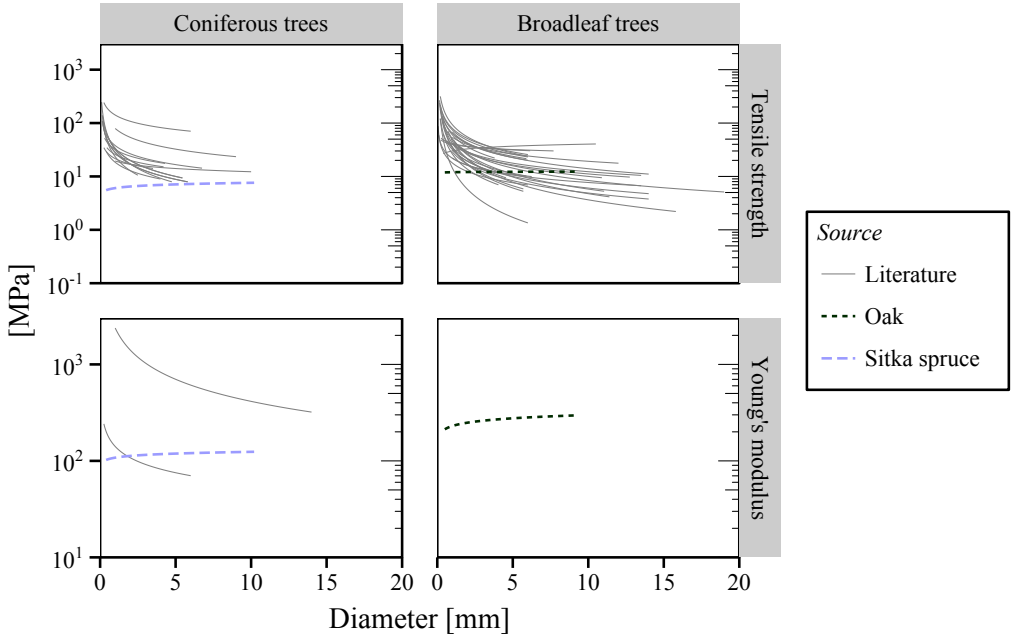

Figure 18: Reported diameter versus tensile strength and tensile stiffness relationships in literature, plus oak and Sitka spruce data from this study. Literature data from Abernethy and Rutherfurd (2001); De Baets et al. (2008); Van Beek et al. (2005); Bischetti et al. (2005, 2009); Burroughs and Thomas (1977); Docker and Hubble (2008); Genet et al. (2005, 2008, 2010); Nilaweera and Nutalaya (1999); Pollen and Simon (2005); Preti (2013); Thomas and Pollen-Bankhead (2010); Waldron and Dakessian (1981).

of 15–63 MPa for 4–10 mm diameter roots and an average Young's modulus of approximately 900 MPa, although these values were calculated using underbark rather than overbark root diameter. Parr and Cameron (2004) found tensile strengths of 35–50 MPa for roots thinner than 2 mm, while O'Loughlin and Ziemer (1982) reported an average tensile strength of 23 MPa for live roots in their decomposition study. These values are higher than found in this study ($3 \leq \sigma_t \leq 14$ kPa). Biomechanical properties are however not only dependent on species and diameter. For example, different root types in barley roots (nodal, seminal or lateral roots) showed significant differences in strength (Loades et al., 2013). Root strength is influenced by root water content (Yang et al., 2016), root age (Genet et al., 2008) or soil conditions such as moisture content (Loades et al., 2013). Furthermore, the shape and internal structure of tree roots was found to adapt to environmental loading conditions such as wind loading (Nicoll and Ray, 1996), likely introducing additional variation in biomechanical properties.

For other tree species than investigated in this study, almost all reported diameter–tensile strength power coefficients for tree species are negative (Figure 18), in contrast to the values found in this study. A notable exception is data on Norway spruce (*Picea abies*) reported by Vergani et al. (2014) with power coefficients ranging between $-0.17 \leq \alpha_\sigma \leq 0.13$, depending on the sampling site (original fits reported in terms of force). However, none of these studies report statistical significance of their fitting parameters. All of the tested roots were woody. Possible explanations for the increased strength and stiffness of roots with larger diameters are: 1) thicker roots are generally older, and therefore stronger or denser tissue might have developed; 2) the ratio of bark area over stele area might be higher for thicker roots. Since strength and stiffness parameters were determined using the overbark diameter, this might result in higher apparent strength or stiffness values in thicker roots.

Both predictive models assume that root cross sections are homogeneous, i.e. strength and stiffness are equally distributed. However, tensile testing showed that both are concentrated in the lignified stele of the root. The bending model assumed that the root fails when the strength of the outermost

point of the cross-section is exceeded (i.e. elastic beam theory). While this type of failure was observed during 3-point bending tests on thick oak roots, rupturing in tension on the convex side, this was not observed for Sitka spruce roots. Instead, Sitka spruce roots buckled, explaining why the bending model does not work well on Sitka roots. This indicates that it is important to study the effects of root structure and biomechanics in more detail, as the root structure might govern the failure mode of roots under penetrometer loading and therefore define the most appropriate interpretative model to use. Thin root diameters ($d_r \leq 2$ mm) broke in tension regardless of tree species. A possible explanation is that the axial stress in a circular beam or rod increases linearly with quadratic increases in diameter (power two), but the bending stress with power three. Therefore it is more likely that small diameter roots will be loaded to failure in tension more than thicker roots.

Root diameters predicted using peak root resistance were more accurate than those predicted by peak root displacement. These results correspond with the results found for penetrometer testing with ABS root analogues in dry sand (Meijer et al., 2017), where the peak root resistance could be predicted much more accurately than the displacement required to reach this peak. In addition, laboratory predictions for root displacement were much more accurate in the laboratory than in the field. Multiple explanations for these observations are possible:

1) In the field, peak root displacement was more difficult to determine from the resistance trace than peak root resistance, introducing inaccuracies. For many root peaks, especially in the Sitka spruce forest, the peak root displacement could not be accurately determined resulting in a smaller dataset. Furthermore, some root peaks might have overlapped, resulting in a potential underestimation of u_u and therefore a smaller predicted root diameter. 2) For both interpretative models, diameter predictions based on peak root displacement are more sensitive to variations in root strength, root stiffness and soil resistance compared to predictions based on peak root resistance (compare equations 3 and 4 or 5 and 6). While previous tests in the laboratory were highly controllable (root analogues and dry sand), the field results presented in this paper show that both root biomechanical properties and soil resistance with depth are highly variable. 3) Peak root displacement depends greatly on assumed soil resistance p_u in both bending and cable models. The method for estimating p_u from the experimentally measured depth-penetrometer resistance traces introduced many uncertainties, e.g. the assumed ratio between standard penetrometer resistance and resistance against root displacement (α_2) or the assumption that the penetrometer resistance just after a force drop is equivalent to the penetrometer resistance in fallow soil. The latter assumption supposes that all penetrometer resistance after a root breakage is caused by the soil rather than other (yet unbroken) roots or debris, which might not always be true.

In the Sitka spruce forest, many sudden drops in penetrometer resistance were found which could not be associated with nearby roots, but were found in layers containing lots of gravel. This site had a higher gravel content than the oak forest (Figure 2) and suggests that stones might influence the test results. The results for the oak forest suggest that using microphones can provide an additional independent measurement and might prove to be a useful tool in addressing this problem. Some of the sudden drops in penetrometer resistance were accompanied by short duration burst in sound amplitude, indicating a root failure event. It is expected that stones will show a longer duration, scraping noise. However, because the oak forest did not contain large amounts of gravel this hypothesis could not be verified.

Because of the difficulties involved in root sampling after testing, it could not always be precisely established which root corresponded to which root peak. Often each root could potentially be associated with several root peaks and vice versa. A decision had to be made based on visual observations and logic (e.g. when two roots could be associated with two root peaks, the largest root was related to the largest peak). This introduced an element of subjectivity into the interpretation process and made validation of the measurement technique and the interpretive prediction models less reliable. These problems do not necessarily stem from the interpretive models or penetrometer device, but from difficulties analysing the tested soil to find out the depths and diameters of roots broken by the penetrometer. Future work should therefore focus on the development of more reliable methods

to identify unequivocally which root corresponds to which force drop. In the laboratory, this might be possible by employing X-ray CT scanning during testing. In the field this will be more difficult. Potential methods might be 1) freezing the ground with subsequent block sampling, or 2) filling the penetrometer hole with resin or plaster to fix broken root ends in place, followed by block sampling.

The blade penetrometer was small, limiting its use to roots thinner than approximately 10 mm. The portable experimental apparatus allowed a maximum penetration depth of 0.5 m. However, the apparatus and methodology can easily be scaled up to accommodate larger blades (to test thicker roots) or to reach larger depths. A larger device might be mounted on an all-terrain vehicle to aid field accessibility, although using larger blades increases the chance multiple roots will be loaded simultaneously, potentially complicating data analysis.

This research shows that it is possible to detect roots and their characteristics using a blade penetrometer. The sudden decrease in penetrometer resistance associated with root failure will enable quick estimates of the spatial distribution of root-reinforcement. Further development of this methodology should focus on 1) applying this method to more soil and root types; 2) investigating the influence of root anatomy on its mechanical behaviour, to understand when roots fail, especially in bending; 3) more accurate identification of which root belongs to which measured root peak in the penetrometer resistance trace; 4) developing a robust method to distinguish between sudden decrease in penetrometer resistance caused by root breakages or those caused by stones. For this purpose, sound recording using microphones appears promising; and 5) studying the potential to scale up the device to test thicker and deeper roots.

5 Conclusions

- The diameter of roots broken during installation of the blade penetrometer can be estimated with reasonable accuracy from the sudden decrease in penetration resistance, given a good estimate of root strength, stiffness and soil resistance.
- Diameter predictions made using the penetrometer displacements required to break a root show much more scatter and are less accurate than those based on increased penetrometer resistance. Predictions made using displacements and the assumption roots break in bending were highly inaccurate. Predictions of root diameter based on root displacements are therefore best avoided in field conditions.
- For the two sites and species tested, the analytical cable model provided the best results overall, indicating that roots failed in tension rather than bending (especially Sitka spruce roots). The results for Oak roots thicker than roughly 2 mm however fall between tension and bending predictions, suggesting a more complicated failure mechanism. The contrast between oak and Sitka root behaviour could be attributed to biomechanical differences observed during 3-point bending tests in the laboratory. These differences showcase the importance of root biomechanics.
- In the oak forest, the breakage of roots could be detected from sound recordings made during penetration. This might be a useful, cheap and simple additional tool to distinguish between root breakages and other artefacts affecting the depth–penetration trace.
- The blade penetrometer, combined with interpretative models, can be a straightforward method to assess the distribution, depths and diameters of roots without the requirement for extensive excavation. Tests are quick to perform. However, more calibration work and a better understanding of the root behaviour is required.

Acknowledgements

The authors thank David Boldrin (University of Dundee/James Hutton Institute) for his assistance during the field work. G. J. Meijer acknowledges a studentship provided by Forest Research, funded

by ClimateXChange, the Scottish Government's Centre for Expertise on Climate Change. The James Hutton Institute receives funding from the Scottish Government. The authors thank the manuscript reviewers for their helpful comments.

Notation

$A_{std\,tip}$ - Standard penetrometer tip area [mm^2]
d_r - Root diameter [mm]
E - Young's modulus [MPa]
$E_{90,b}$ - Secant bending stiffness at 90% of peak bending strength [MPa]
$E_{90,t}$ - Secant tensile stiffness at 90% of peak tensile strength [MPa]
E_b - Bending stiffness [MPa]
E_t - Tensile stiffness [MPa]
f - Ratio between soil shear strength and soil–root interface friction [-]
F_{blade} - Blade penetrometer resistance [N]
F_u - Peak root resistance [N]
$F_{u,b}$ - Peak root resistance according to the analytical bending model [N]
$F_{u,t}$ - Peak root resistance according to the analytical cable model [N]
p_u - Ultimate soil resistance against lateral root displacement [MPa]
q_c - Standard penetrometer resistance [MPa]
u_u - Maximum root lateral displacement corresponding with root failure [mm]
$u_{u,b}$ - Maximum root lateral displacement corresponding with root failure according to the analytical bending model [mm]
$u_{u,t}$ - Maximum root lateral displacement corresponding with root failure according to the analytical cable model [mm]
z - Root depth [mm]
α - Fitting parameter in root diameter–strength/stiffness fits
α_1 - Ratio between blade and standard penetrometer resistance force [-]
α_2 - Ratio between root lateral resistance and standard penetrometer resistance [-]
α_E - Fitting parameter in root diameter–stiffness fit
α_σ - Fitting parameter in root diameter–strength fit
β_E - Fitting parameter in root diameter–stiffness fit
β_σ - Fitting parameter in root diameter–strength fit
ζ - Dimensionless parameter in analytical cable model [-]
η - Dimensionless parameter in analytical cable model [-]
σ_b - Peak strength in bending [MPa]
σ_t - Peak strength in uniaxial tension [MPa]
τ_i - Root–soil interface friction [kPa]
τ_{sv} - Shear vane peak strength [kPa]

References

B. Abernethy and I. D. Rutherfurd. The distribution and strength of riparian tree roots in relation to riverbank reinforcement. *Hydrological Processes*, 15(1):63–79, 2001.

G. B. Bischetti, E. A. Chiaradia, T. Simonato, B. Speziali, B. Vitali, P. Vullo, and A. Zocco. Root strength and root area ratio of forest species in Lombardy (northern Italy). *Plant and Soil*, 278 (1–2):11–22, 2005.

Gian Battista Bischetti, Enrico Antonio Chiaradia, Thomas Epis, and Emanuele Morlotti. Root cohesion of forest species in the Italian Alps. *Plant and Soil*, 324(1-2):71–89, 2009.

British Standards Institution. *BS ISO 13320:2009: Particle size analysis. Laser diffraction methods.* British Standards Institution, London, 2010.

E. R. Burroughs and B. R. Thomas. *Declining root strength in Douglas-fir after felling as a factor in slope stability, Research Paper INT-190.* US Department of Agriculture Forest Service, Ogden, Utah, 1977.

N. Coppin and I. Richards. *Use of vegetation in civil engineering, CIRIA book 10.* Butterworths, Kent, 1990.

M. P. Coutts. Root architecture and tree stability. *Plant and Soil*, 71(1–3):171–188, 1983.

S. De Baets, J. Poesen, B. Reubens, J. Wemans, K. De Baerdemaeker, and B. Muys. Root tensile strength and root distribution of typical Mediterranean plant species and their contribution to soil shear strength. *Plant and Soil*, 305(1):207–226, 2008.

B. B. Docker and T. C. T. Hubble. Quantifying root-reinforcement of river bank soils by four Australian tree species. *Geomorphology*, 100(3–4):401–418, 2008.

Chia-Cheng Fan and Chih-Feng Su. Role of roots in the shear strength of root-reinforced soils with high moisture content. *Ecological Engineering*, 33(2):157–166, 2008.

Forestry Commission. *Forestry Statistics 2015 – A compendium of statistics about woodland, forestry and primary wood processing in the United Kingdom.* Forestry Commission, Edinburgh, 2015.

M. Genet, A. Stokes, F. Salin, S. Mickovski, T. Fourcaud, J. F. Dumail, and R. van Beek. The influence of cellulose content on tensile strength in tree roots. *Plant and Soil*, 278(1–2):1–9, 2005.

Marie Genet, Nomessi Kokutse, Alexia Stokes, Thierry Fourcaud, Xiaohu Cai, Jinnan Ji, and Slobodan Mickovski. Root reinforcement in plantations of *Cryptomeria japonica* D. Don: effect of tree age and stand structure on slope stability. *Forest Ecology and Management*, 256(8):1517–1526, 2008.

Marie Genet, Alexia Stokes, Thierry Fourcaud, and Joanne E. Norris. The influence of plant diversity on slope stability in a moist evergreen deciduous forest. *Ecological Engineering*, 36(3):265–275, 2010.

Donald H. Gray and Robbin B. Sotir. *Biotechnical and soil bioengineering slope stabilization, a practical guide for erosion control.* John Wiley & Sons Inc, New York, 1996.

R. B. Jackson, J. Canadell, J. R. Ehleringer, H. A. Mooney, O. E. Sala, and E. D. Schulze. A global analysis of root distribution for terrestial biomes. *Oecologica*, 108(3):389–411, 1996.

James Hutton Institute. Soil information for Scottish soils (SIFFS), 2016. URL http://sifss.hutton.ac.uk/.

K. Lauder. *The performance of pipeline ploughs.* PhD thesis, University of Dundee, 2010.

K. W. Loades, A. G. Bengough, M. F. Bransby, and P. D. Hallett. Planting density influence on fibrous root reinforcement of soils. *Ecological Engineering*, 36(3):276–284, 2010.

K. W. Loades, A. G. Bengough, M. F. Bransby, and P. D. Hallett. Biomechanics of nodal, seminal and lateral roots of barley: effects of diameter, waterlogging and mechanical impedance. *Plant and Soil*, 370(1):407–418, 2013.

Zhun Mao, Laurent Saint-Andre, Marie Genet, Francois-Xavier Mine, Christophe Jourdan, Herve Rey, Benoit Courbaud, and Alexia Stokes. Engineering ecological protection against landslides in diverse mountain forests: Choosing cohesion models. *Ecological Engineering*, 45:55–69, 2012.

G. J. Meijer, A. G. Bengough, J. A. Knappett, K. W. Loades, and B. C.. Nicoll. New in-site techniques for measuring the properties of root-reinforced soil – laboratory evaluation. *Géotechnique*, 66(1): 27–40, 2016.

G. J. Meijer, A. G. Bengough, J. A. Knappett, K. W. Loades, and B. C.. Nicoll. In situ root identification through blade penetrometer testing – part 1: interpretative models and laboratory testing. *Géotechnique*, 2017. Under review.

S. B. Mickovski, P. D. Hallett, M. F. Bransby, M. C. R. Davies, R. Sonnenberg, and A. G. Bengough. Mechanical reinforcement of soil by willow roots: Impacts of root properties and root failure mechanism. *Soil Science Society of America Journal*, 73(4):1276–1285, 2009.

B. C. Nicoll and D. Ray. Adaptive growth of tree root systems in response to wind action and site conditions. *Tree Physiology*, 16(11–12):891–898, 1996.

N. S. Nilaweera and P. Nutalaya. Role of tree roots in slope stabilisation. *Bulletin of Engineering Geology and the Environment*, 57(3):337–342, 1999.

Colin O'Loughlin and Robert R. Ziemer. The importance of root strength and deterioration rates upon edaphic stability in steepland forests. In *I.U.F.R.O. Workshop P.1.07-00 Ecology of Subalpine Ecosystems as a Key to Management*, pages 70–78, Courvallis, Oregon, 1982. Oregon State University.

V. Operstein and S. Frydman. The influence of vegetation on soil strength. *Ground Improvement*, 4: 81–89, 2000.

A. Parr and A. D. Cameron. Effects of tree selection on strength properties and distribution of structural roots of clonal Sitka spruce. *Forest Ecology and Management*, 195(1–2):97–106, 2004.

N. Pollen and A. Simon. Estimating the mechanical effects of riparian vegetation on stream bank stability using a fiber bundle model. *Water Resources Research*, 41(7):W07025, 2005.

F. Preti. Forest protection and protection forest: Tree root degradation over hydrological shallow landslides triggering. *Ecological Engineering*, 61, Part C:633–645, 2013.

Lymon C. Reese and William F. Van Impe. *Single piles and pile groups under lateral loading, 2nd edition*. CRC, Leiden, The Netherlands, 2011.

Nicholas P. Rowe, Sandrine Isnard, Friederike Gallebmüller, and Thomas Speck. Diversity of mechanical architectures in climbing plants: an ecological perspective. In Anthony Herrel, Thomas Speck, and Nicholas Rowe, editors, *Ecology and biomechanics: a mechanical approach to the ecology of animals and plants*, pages 35–60. CRC, Boca Raton, FL, US, 2006.

Alexia Stokes, Claire Atger, Anthony Glyn Bengough, Thierry Fourcaud, and Roy C. Sidle. Desirable plant root traits for protecting natural and engineered slopes against landslides. *Plant and Soil*, 324 (1–2):1–30, 2009.

Robert E. Thomas and Natasha Pollen-Bankhead. Modeling root-reinforcement with a fiber-bundle model and Monte Carlo simulation. *Ecological Engineering*, 36(1):47–61, 2010.

L. P. H. Van Beek, J. Wint, L. H. Cammeraat, and J. P. Edwards. Observation and simulation of root reinforcement on abandoned Mediterranean slopes. *Plant and Soil*, 278(1–2):55–74, 2005.

C. Vergani, M. Schwarz, D. Cohen, J. J. Thormann, and G. B. Bischetti. Effects of root tensile force and diameter distribution variability on root reinforcement in the Swiss and Italian Alps. *Canadian Journal of Forest Research*, 44(11):1426–1440, 2014.

L. J. Waldron and S. Dakessian. Soil reinforcement by roots – calculation of increased soil shear resistance from root properties. *Soil Science*, 132(6):427–435, 1981.

Yuanjun Yang, Lihua Chen, Ning Li, and Qiufen Zhang. Effect of root moisture content and diameter on root tensile properties. *PLoS ONE*, 11:1–17, 2016. doi: 10.1371/journal.pone.0151791.